A Luminescent Probe of Mismatched DNA Hybridization: Location and Number of Mismatches

*Amira F. El-Yazbi[ab], Alysha Wong[a], and Glen R. Loppnow[a]**

[a] Department of Chemistry, University of Alberta, Edmonton, AB T6G 2G2, Canada

[b] Department of Pharmaceutical Analytical Chemistry, Faculty of Pharmacy, Alexandria University, Alexandria, Egypt

* Corresponding author. Tel.: (780) 492-9704; Fax: (780) 492-8231.

e-mail address: glen.loppnow@ualberta.ca (G. R. Loppnow).

Abstract

The human genome is susceptible to change; base mismatches can arise from damaged DNA, replication errors, and spontaneous mutation, and have the potential to cause apoptosis, carcinogenesis, and mutagenesis. Many techniques have been developed for DNA mismatch detection, but many of these methods have complex, time-consuming procedures and are limited to the detection of specific types of DNA mismatches. In this work, we present a general method for the simple and sensitive nucleobase-sensitized luminescent detection of mismatches in double-stranded DNA (dsDNA) using terbium ions. Terbium ions luminesce differently depending on the site of coordination in DNA due to the proximity effect of the energy transfer

process that occurs from excited, non-hydrogen bonded nucleobases in single-stranded DNA (ssDNA) regions to the terbium ions. We examined the effect of location and number of mismatches on the sensitivity and selectivity of this probe in both synthetic oligonucleotides containing mismatches and natural calf thymus DNA exposed to UV light to induce reduced base pairing due to damage. This method shows good sensitivity for the determination of DNA mismatches, with limit of detection and limit of quantification of 1 and 3 mismatches, respectively, per dsDNA sequence.

Keywords

Terbium, Luminescence, DNA mismatch detection, Nucleic acids, UV-induced DNA damage, DNA probe.

1. Introduction

The human genome consists of about 6 billion nucleobases[1] forming genes that are replicated each time a cell divides. It is estimated that natural mutations are introduced at the frequency of 1 in 10^7 nucleotides due to the inherent accuracy of DNA polymerase, the enzyme responsible for adding nucleotides during the replication of DNA [1]. A proposed hypothesis suggests that another cause of spontaneous mutation may be the tautomeric shifts of bases from the "keto" forms required for the correct Watson & Crick base pairing to their rarer "imino" or "enol" forms. As a result, adenine pairs with the tautomer of cytosine and thymine pairs with the guanine tautomer, resulting in base-pair mismatches [2-4]. DNA in cells is also susceptible to damage from various other sources, such as reactive oxygen species (ROS) resulting from different metabolic processes leading to oxidative damage,

exposure to ultraviolet (UV) radiation leading to photoproducts, chemicals leading to adducts, and ionizing radiation leading to single- and double-strand breaks [5]. Similar to natural and spontaneous mutation, DNA damage may also lead to base-pair mismatches, resulting in mutagenesis, carcinogenesis or cell death [6-9].

Various techniques have been developed for detecting mismatched and damaged DNA, including DNA sequencing [10], enzymatic analysis [11,12] and gravimetric analysis [13,14]. Separation techniques have also been developed to detect mismatched DNA, including high performance liquid chromatography (HPLC) [15-17], capillary electrophoresis [18,19] and gel electrophoresis [20,21]. All these techniques are able to assess damaged and mismatched DNA, however they all also require complex, elaborate and time-consuming procedures for the selective determination of the damaged or mismatched sites [10-21].

To reduce this limitation, chromatography-free techniques involving DNA hybridization and fluorescence have been developed to detect mismatches [22]. Fluorescence techniques offer higher sensitivity than other techniques, since they have a zero background. Examples of these combined hybridization/fluorescence techniques include molecular beacons [23-28] and fluorescent-tagged oligonucleotides [29-31]. Both molecular beacons and fluorophore-labelled oligonucleotides rely on hybridization for damage detection and a consequent change in the fluorescence signal for reporting the amount of damage [23-28].

Recently, luminescent terbium(III) chloride (Tb^{3+}) has been used for the detection of damaged DNA [32,33]. Tb^{3+} possesses low intrinsic luminescence in aqueous solutions

owing to its low absorption cross-section and non-radiative deactivation through the OH vibrations of the coordinated water molecules [32-34]. In the presence of dsDNA, one or more of the waters may be replaced by the deprotonated oxygen of the phosphate group making up the backbone of the DNA, but no change in the emission properties is observed because no energy transfer-enhancing coordination between Tb^{3+} and the already base-paired nucleobases can occur [32, 34]. However, upon chelation of the ion by the lone electron pairs of unpaired nucleobases in ssDNA, Tb^{3+} emission is enhanced 2-3 times by radiationless energy transfer from the excited nucleobase [32-34]. In this process, the excited nucleobase undergoes intersystem crossing from the excited singlet state of the unpaired nucleobases to its excited triplet state, followed by radiationless energy transfer from that excited triplet state to the overlapping resonance energy levels of Tb^{3+}. This process leads to both longer emission lifetimes and greater absorption of the incident light by the more absorbing nucleobases, leading to this Tb^{3+} luminescence enhancement. This enhancement makes Tb^{3+} a selective probe for unpaired regions of DNA [32-38]. The energy gap between Tb^{3+}'s lowest excited, emissive state and its ground state, 14800 cm^{-1}, yields significant visible emission intensity, as compared to other lanthanide ions [38]. Tb^{3+} already has a wide range of applications; it has been used as a probe for DNA damage [33], an optical sensor for DNA and chromatin [35], and a probe for studying drug-DNA interactions [39]. Tb^{3+} is biologically inert [40,41], unlike many organic fluorophores, giving this technique potential for *in vivo* applications and the fact that the mechanism only involves changes in coordination, this technique also has potential for *in situ* determination of hybridization, such as in RT-PCR.

In this paper, we explore the enhanced emission of Tb^{3+} ions as a potential spectroscopic biosensor for the selective and sensitive detection of DNA base mismatches. Enhancement of Tb^{3+} emission upon binding to synthetic oligonucleotides with pre-determined amounts and locations of mismatches, as well as in determining the amount of UVC-induced damage in calf thymus DNA has been explored. Results show that Tb^{3+} luminescence is sensitive for single-base mismatch detection, and that the luminescence increases as the number of mismatches in dsDNA increases, although the correlation is complicated by location effects. Also, higher luminescence enhancement is obtained from UVC-damaged calf thymus DNA samples, while no luminescence enhancement is obtained from undamaged samples. Such a probe is a simple, selective and sensitive biosensor for the detection of damaged or mismatched sites in nucleic acids, solving many of the issues with other methods of detecting mismatches.

2. Experimental

2.1. Materials

Single- and double-stranded oligonucleotide targets, mismatched targets and the hairpin probe (sequences in Tables 1 and 2) were all purified by standard desalting and were obtained from Integrated DNA Technologies Inc. (Coralville, Iowa). The calf thymus DNA (ctDNA) and the terbium(III) chloride were obtained from Sigma-Aldrich Canada Ltd. (Oakville, Ontario), sodium chloride was obtained from EMD Chemicals Inc. (Gibbstown, New Jersey), and Tris was obtained from ICN Biomedicals (Aurora, Ohio). All chemicals were used as received. Nanopure water from a Barnsted Nanopure (Boston, Massachusetts) system was used for all solutions. The oligonucleotide samples and hairpin probe were each

diluted in nanopure water to a final concentration of 20 μM and kept frozen at –20 °C until needed.

2.2. Instrumentation

Absorption spectra were recorded on an Agilent 8453 diode array spectrophotometer. The fluorescence measurements were done using a Photon Technologies International (Birmingham, New Jersey) fluorescence spectrophotometer. The ctDNA was irradiated in a Luzchem (Ottawa, Ontario) DEV photoreactor chamber with UVC light from six lamps emitting principally at 254 nm, each with an output of 75 W m^{-2}.

2.3. Procedures

2.3.1. Sample hybridization

Aliquots of the ssDNA targets were mixed with appropriate amounts of the hairpin probe (hp) and buffer solution to give final concentrations of 2 μM oligonucleotide targets and 2 μM hairpin probes (40 mM Tris, 10 mM NaCl, pH 7.5). These solutions were heated to 85ºC in a water bath and then annealed at room temperature (25°C) in the dark for 24 hr to assure complete hybridization. Similarly, 1 μM dsDNA samples in buffer (40 mM Tris, 10 mM NaCl, pH 7.5) were gradually heated to 85°C in a water bath and annealed twice at room temperature (25°C) in the dark for 24 hr. For ctDNA, a 10 μg/mL solution was prepared in buffer (40 mM Tris, 10 mM NaCl, pH 7.5) and left for 24 hr at room temperature to completely dissolve.

2.3.2. UV irradiation

Nitrogen-purged solutions of 10 μg/mL ctDNA in buffer (40 mM Tris, 10 mM NaCl, pH 7.5) were irradiated with UVC light in sealed, UV-transparent 1 cm pathlength cuvettes. The cuvettes were placed in a water bath in a UV-transparent water dish to keep the temperature constant throughout the irradiation. The samples were constantly stirred during irradiation, and the photoreactor was purged with nitrogen throughout the irradiation to flush out oxygen and any ozone subsequently generated from the UVC lamps. Control samples were handled identically, but were not exposed to UV radiation. The UVC lamps were turned on 20 min before the start of irradiation to stabilize the lamp output.

2.3.3. Luminescence measurements

Prior to the luminescence measurements, $TbCl_3$ solution was added to the hybridized 17-oligmer ssDNA-hp solutions to a final concentration of 40 μM Tb^{3+} and 1 μM ssDNA-hp, while $TbCl_3$ solution was added to the 90-oligomer dsDNA solutions to a final concentration of 90 μM Tb^{3+} and 0.5 μM dsDNA. For the luminescence measurements of the irradiated ctDNA, a 10 μL aliquot of the irradiated solution was taken at various time intervals, to which Tb^{3+} solution was added and mixed with buffer (40 mM Tris, 10 mM NaCl, pH 7.5) to give final concentrations of 1 μg/mL ctDNA and 3 mM Tb^{3+}. Luminescence spectra between 450 and 650 nm with excitation at 280 nm of 100 μL aliquots of such solutions in a 1 cm path length Suprasil quartz fluorescence cuvette were measured.

In order to optimize the Tb^{3+} luminescence detection of mismatches, we examined the effect of buffer and sodium ion concentrations on Tb^{3+} luminescence. Results

(supplementary material) show that 10 mM Na^+ and no Mg^{2+} ions in buffer r (40 mM Tris, 10 mM NaCl, pH 7.5) gave the maximum luminescence enhancement in the presence of ssDNA and were further used for all subsequent measurements.

3. Results and discussion

Scheme 1 outlines the rationale for this experiment. Briefly, the change from dsDNA to ssDNA in whole or in part leads to a change in the binding site of Tb^{3+} ions; in dsDNA, the Tb^{3+} ions act as counterions to the phosphate negative charges at physiological pH. In ssDNA, however, the Tb^{3+} ions are more likely thermodynamically to bind to the nitrogenous nucleobases [32-34]. Once bound to these nucleobases, they are more luminescent due to energy transfer, particularly with guanine. Thus, an increase in luminescence intensity is a marker for some ssDNA tracts within the oligomers.

Figure 1 compares the 280 nm-excited luminescence spectra of a mixture of Tb^{3+} and ssDNA sequence S^0 in the absence and presence of the hairpin (hp) probe (Table 1). As shown in Figure 1, the Tb^{3+} luminescence is significantly lower in the presence of the ssDNA-hp hybrid compared to the ssDNA alone. This result is consistent with what was observed previously with linear strands of other sequences of ssDNA and dsDNA [32,33]. The major luminescent peaks of the Tb^{3+} complex, centered at 490, 546, 586, and 622 nm, originate from the $^5D_4 \rightarrow {}^7F_J$ (J = 6, 5, 4, 3, respectively) transitions, with the strongest emission located at 546 nm. At the 546 nm peak, the difference in luminescence intensity between ssDNA and the hybrid is the greatest. The luminescence intensity increase in the presence of ssDNA has been attributed to energy transfer from the unpaired nucleobases to

the Tb^{3+} ion when Tb^{3+} is bound to the free electron pairs of the nucleobases [32,33], in addition to changes in the coordination sphere of the Tb^{3+} ion [34]. It was previously reported that the lanthanide ion loses one water molecule in the presence of dsDNA, while it loses six water molecules with ssDNA due to its binding to the free nucleobases [34].

3.1. Selectivity of Tb^{3+} luminescence to mismatches

To examine the effect of mismatch location on hybridization, 14 ssDNA 17-mer oligonucleotides were used with 0-4 mismatches in various locations, in addition to a single hp probe that was used as the complementary strand for all oligomers. Table 1 shows the sequences of the oligomers used. The location of mismatches are central (positions 8 and 9), semi-central (positions 5 and 13), semi-terminal (positions 3 and 15) or terminal (positions 1 and 17).

The sequence of the hp probe used in this study is also presented in Table 1. The stem consists of six self-complementary bases at either end of the sequence. The stem sequence is responsible for the hairpin formation in the absence of the complementary ssDNA. If ssDNA complementary to the loop is present, the hairpin will bind to that, effectively destroying the self-complementary base-pairing of the stem. The hp probe is designed to detect mismatches because the stem melting temperature (T_m), the temperature necessary to dissociate 50% of the base pair hydrogen bonding, is 5 – 10 °C higher than the T_m of the hybrid [23-26]. The hp probe hybridizes best with the perfect DNA complement. With mismatched sequences, the ssDNA-hp hybrid is more unstable, leading to a greater proportion of the probe in the hairpin structure and the mismatched ssDNA sequence unhybridized. Upon addition of Tb^{3+}, the luminescent ion directly coordinates to the

unpaired nucleobases of the unhybridized ssDNA. As described above, excitation of such nucleobases in the DNA enhances the intrinsic luminescence of Tb^{3+} via energy transfer to the coordinated Tb^{3+} ions with a signal that should be directly proportional to the number of mismatches present.

Figure 2 shows the Tb^{3+} luminescence signal as a function of location and number of mismatches in the DNA target. In general, the results show both a location- and number-dependence of the luminescence intensity. It is expected that regions where mismatches are located will likely be more accessible to binding of the Tb^{3+} ions to the free nucleobases, leading to greater luminescence. Thus, Tb^{3+} luminescence should be directly proportional to the amount of mismatches present in oligoDNA. Figure 2 shows that the luminescence signal is very small for sequence S^0 binding to the hp probe. This is attributed to the fact that the S^0-hp duplex is perfectly complementary, with little or no ability for Tb^{3+} ions to bind to free nucleobases.

Upon comparing strands with only one mismatch, the results in Figure 2 show that the oligonucleotide with a mismatch located at the center of the oligomer, S_8^1, exhibited the most Tb^{3+} luminescence enhancement of all the sequences. Sequences with single-base mismatches located at semi-central (S_5^1 and S_{13}^1) and semi-terminal (S_3^1, S_{15}^1) sites had lower Tb^{3+} luminescence enhancement, and sequences with a mismatch located at the terminal positions (S_1^1 and S_{17}^1) had the lowest luminescence enhancement of all single mismatch sequences. It is worth noting that, although the terminal mismatches produced lower luminescence enhancement than the other locations, Figure 2 shows that the enhancement obtained is still much higher than that of the hybrid between S^0 and hp. This result

demonstrates that the Tb^{3+} ion produces good discrimination between the perfect ssDNA-hp hybrid and the single-base mismatched duplexes. This result also suggests that mismatches in the center of oligonucleotide duplexes may differentially destabilize the duplex more than mismatches at the termini, where the duplex is already flexible and may promote some transient Tb^{3+}-nucleobase coordination even when perfectly complementary. This agrees with the previous findings of the significant effect of mismatch position on duplex stability rather than the mismatch type [42,43].

Similarly, upon comparing strands with two mismatches, Figure 2 shows that the highest Tb^{3+} luminescence enhancement was obtained from the sequence with two central mismatches, $S^2_{8,9}$, while the strand with two terminal mismatches, $S^2_{1,17}$, produced the lowest enhancement. On the other hand, strands with four mismatches obtained comparable high luminescence regardless of the location of the mismatches.

The correlation of changes in luminescence intensity with the number and location of mismatches reflect the structural changes within the dsDNA where the unpaired mismatched bases are not as stacked in the double helical structure as the paired bases are showing higher relative dynamics at the site of mismatches. This has recently been reported to be the trigger for mismatch repair pathways [44-46]. Recent findings indicate that the orthologous enzyme of NucS, an endonuclease, is a mismatch-specific enzyme. It specifically cleaves dsDNA containing single-base mismatches [44,45] and the mismatched bases were flipped out into the enzyme binding sites [44].

3.2. Sensitivity of Tb^{3+} luminescence to number of mismatches

In order to investigate the sensitivity of the Tb^{3+} luminescence to detect DNA

mismatches and their effect on DNA hybridization, 26 double-stranded 90-mer oligonucleotide sequences were designed with 2 to 88 central mismatches. The dsDNA helical structure is stabilized by both base stacking and base pairing, and the T_m reflects the overall stability of the dsDNA. The higher the number of mismatches, the greater the instability of the double helix due to weaker hydrogen bonding between Watson-Crick base-pairs (A•T and C•G), and the lower the T_m of the double strand. Figure 3A presents the calculated [47] T_m's of the different mismatched dsDNA sequences versus the number of mismatches present in each sequence. As shown in Figure 3A, the T_m generally decreases with increasing number of mismatches due to the decreasing stability of the duplex DNA. The sequence with no DNA mismatches (D^0) has a T_m of 75.9 ^oC. Upon increasing the number of mismatches, the T_m decreases gradually, until it is 47.4 ^oC for the sequence with 72 DNA mismatches. However, increasing the number of mismatches over 72 leads to a much larger drop in the T_m. This result reflects the severe destabilization that occurs after 72 central mismatches in a dsDNA sequence of 90 base pairs. Also, it is worth noting that sequences with 78 or more DNA mismatches have T_m's calculated to be below zero ^oC, i.e. at room temperature. It is expected that such duplexes will be completely melted into their single-stranded oligomer components.

Consequently, in order to study the sensitivity of the Tb^{3+} luminescence to detect DNA mismatches, we have selected eleven 90-mer dsDNA sequences (Table 2) from those plotted in Figure 3A. Figure 3B shows a plot of the Tb^{3+} luminescence as a function of the number of mismatches in these dsDNA sequences. In Figure 3B, minimum luminescence is obtained with the perfectly complementary duplex, i.e. zero DNA mismatches, as all the

nucleobases are involved in hydrogen bonding and cannot enhance Tb^{3+} luminescence. Upon increasing the number of mismatches in the dsDNA, the Tb^{3+} luminescence gradually increases due to the decreased stability of the dsDNA hybrid and greater base-Tb^{3+} coordination, enhancing the Tb^{3+} luminescence. Although some of this luminescence increase may be due to Tb3+ ions complexing with unpaird hp, this luminescence value was difficult to determine, as the amount of unpaired hp will vary with the number of mismatches. We estimate that this luminescence is less than 10% of the observed increase at the maximum number of mismatches. Tb^{3+} luminescence reaches its maximum for the dsDNA sequence with 72 mismatches after which the Tb^{3+} luminescence remains essentially constant for sequences with mismatches more than 72, consistent with the T_m calculations and measurements in Figure 3A. This plateau indicates that 90-mer oligonucleotide sequences with 72 mismatches or more, i.e. $\geq$ 80% mismatches, cause essentially complete destabilization of the duplex. Table 3 shows the analytical figures of merit for the quantification of mismatch number in dsDNA from Figure 3B. Good sensitivity was obtained with a limit of detection (LOD) and a limit of quantitation (LOQ) of 1 and 3 mismatches, respectively.

In order to confirm the trend of the Tb^{3+} luminescence as a function of number of mismatches, the absorbance at 260 nm of dsDNA sequences with different number of mismatches were also measured (Figure 3C). This measurement relies on the hypochromic absorbance in the ultraviolet absorption spectrum that is observed in duplex DNA due to the better stacking of purine and pyrimidine residues [48,49]. A slight increase in absorbance is observed with an increase in the number of mismatches until it reaches its maximum for

DNA sequences with 72 mismatches, consistent with both the T_m and Tb^{3+} luminescence measurements in Figures 3A and 3B. For sequences having more than 72 mismatches, the absorbance measurements remained constant and were equivalent to the sum of the absorbance of D_{4-87}^{84} and C separately at the same concentration, confirming that 72 mismatches or more in a 90-mer oligonucleotide sequence causes maximum destabilization of the duplex. However, the results in Figure 3B show a linear increase in luminescence intensity with the increase in mismatch numbers, while the results in Figure 3C show an exponential increase in absorbance as the number of mismatches increases. This can be attributed to either the higher sensitivity of the luminescence intensity, which is measured against a zero background compared to the absorbance measurement, or to the inherent different mechanisms of luminescence enhancement and hypochromism. Thus, the T_m and luminescence measurements show similar amounts of duplex destabilization with large mismatch numbers. Consequently, such hybrids are completely unstable and are mostly present as single strands at room temperature.

3.3. Probing UV-induced DNA damage of calf thymus DNA

UVC (200–290 nm) light causes direct damage to DNA and leads to the formation of thymidine cyclobutyl photodimers (CPD) as the primary photoproduct under anoxic conditions [5]. Other photoproducts with UV irradiation are pyrimidine pyrimidinone [6–4] photoproducts, dewar pyrimidinones, and uracil and thymine photohydrates. Most of these photoproducts are localized on the pyrimidine nucleobases near the C5=C6 double bond, opposite to the site of base pairing. However, their presence still affects the duplex structure

and stability [50-52]. The Tb^{3+} luminescence probe, developed in this study, was used to measure the base-pair mismatches formed upon UVC irradiation of calf thymus DNA (ctDNA).

As shown in Figure 4, the Tb^{3+} luminescence increases with UVC exposure time under these conditions until it reaches a plateau after 240 min of irradiation. No change in luminescence is observed for the unirradiated control with increasing time. This result indicates that after 4 hr of UVC light irradiation, the ctDNA sample was completely damaged under the conditions used here and Tb^{3+} exhibited its maximum luminescence enhancement. The luminescence intensity as a function of irradiation time for ctDNA (Figure 4) was fit to a single exponential growth function to obtain a damage constant of 66.42 ± 4.13 min under these conditions.

These results conclusively show that the Tb^{3+} probe is a sensitive tool to detect DNA mismatches. In contrast to other reported methods for DNA mismatch detection [11-27], our proposed method offers many other advantages besides being selective and sensitive to DNA mismatches. For instance, there are no sophisticated or multi-step sample pre-treatment procedures are required prior to luminescence measurements, as is the case in most of the other reported methods [11-19]. Also, the Tb^{3+} probe is added directly to the dsDNA sample without the need for DNA denaturation or PCR amplification steps before chromatographic analysis [15-21]. Such steps add to the complexity and, potentially, the cost of the methods [15-21]. Thus, our method can be used generally for any mismatch detection in DNA, something that other techniques cannot do, such as hybridization probes [23-27], where a specific DNA sequence is required for each sample, or enzymatic analysis [11,12], which requires the use of

specific enzymes to ensure the correct cleavage at the site of mismatch. Finally, the Tb^{3+} probe method provides a convenient, easy and biologically safe technique for the determination of base mismatches in dsDNA. Such a probe represents a promising tool in the design of biosensors for the *in vivo* detection of nucleic acid mismatches and damage.

4. Conclusion

In summary, the assay reported here uses Tb^{3+} luminescence as a biosensor for the quantification of nucleic acid mismatches, by taking advantage of the luminescence enhancement with increasing number of mismatches. This biosensor shows good sensitivity and selectivity for DNA mismatch detection, together with the main advantages of being simple, cheap and readily available. The Tb^{3+} luminescence biosensor has also been successfully applied to the determination of UV-induced damage in calf thymus

Acknowledgements

The authors acknowledge financial support for this work from the Canadian Natural Sciences and Engineering Research Council (NSERC) Discovery Grants-in-aid programme.

References

(1) B. Alberts, A. Johnson, J. Lewis, M. Raff, K. Roberts, P. Walter, Molecular Biology of the Cell, 4th edition, New York: Garland Science, 2002.

(2) W. Wang, H.W. Hellinga, L.S. Beese, Structural evidence for the rare tautomer hypothesis of spontaneous mutagenesis, Proc. Natl. Acad. Sci. U.S.A. 108 (2011) 17644-17648.

(3) A. Sancar, L.A. Lindsey-Boltz, K. Ünsal-Kaçmaz, S. Linn, Molecular mechanisms of mammalian DNA repair and the DNA damage checkpoints, Annu. Rev. Biochem. 73 (2004) 39-85.

(4) J. Wijnen, H. van der Klift, H. Vasen, P.M. Khan, F. Menko, C. Tops, H. Meijers Heijboer, D. Lindhout, P. Moller, R. Fodde, *MSH2* genomic deletions are a frequent cause of HNPCC, Nat. Genet. 20 (1998) 326-328.

(5) S. Kumari, R.P. Rastogi, K.L. Singh, S.P. Singh, R.P. Sinha, DNA damage: detection strategies, EXCLI Journal 7 (2008) 44-62.

(6) B. Ames, L. Gold, W. Willett, The causes and prevention of cancer, Proc. Natl. Acad. Sci. U.S.A. 92 (1995) 5258-5265.

(7) T. Lindahl, Instability and decay of the primary structure of DNA, Nature 362 (1993) 709-715.

(8) L. Marnett, P. Burcham, Endogenous DNA adducts: Potential and paradox, Chem. Res. Toxicol. 6 (1993) 771-785.

(9) L. Marrot, J. Meunier, Skin DNA photodamage and its biological consequences, J. Am. Acad. Dermatol. 58 (2008) S139-S148.

(10) F. Sanger, S. Nicklen, A.R. Coulson, DNA sequencing with chain-terminating inhibitors, Proc. Natl. Acad. Sci. U.S.A. 74 (1977) 5463-5467.

(11) B. J. Till, C. Burtner, L. Comai, S. Henikoff, Mismatch cleavage by single-strand specific nucleases, Nucl. Acids Res. 32 (2004) 2632-2641.

(12) T.E. Shenk, C. Rhodes, P.W.J. Rigby, P. Berg, Biochemical Method for Mapping Mutational Alterations in DNA with SI Nuclease: The Location of Deletions and Temperature-Sensitive Mutations in Simian Virus 40, Proc. Natl. Acad. Sci. U.S.A. 72 (1975) 989-993.

(13) S.O. Kelley, E.M. Boon, J.K. Barton, N.M. Jackson, M.G. Hill, Single-base mismatch detection based on charge transduction through DNA, Nucl. Acids Res. 27 (1999) 4830-4837.

(14) Y. Weizmann, F. Patolsky, I. Willner, Amplified detection of DNA and analysis of single-base mismatches by the catalyzed deposition of gold on Au-nanoparticles, Analyst 126 (2001) 1502–1504

(15) F. Totsingan, T. Tedeschi, S. Sforza, R. Corradini, R. Marchelli, Highly selective single nucleotide polymorphism recogniton by a chiral (5S) PNA beacon, Chirality 21 (2009) 245–253.

(16) A. Roloff, S. Ficht, C. Dose, O. Seitz, DNA-Templated Native Chemical Ligation of Functionalized Peptide Nucleic Acids: A Versatile Tool for Single Base-Specific Detection of Nucleic Acids, Meth. Mol. Biol. 1050 (2014) 131-141.

(17) D.L. Fackenthal, P.X. Chen, S. Das, Denaturing high-performance liquid chromatography for mutation detection and genotyping, Meth. Mol. Biol. 311 (2005) 73-96.

(18) J. Ren, A. Ulvik, H. Refsum, P.M. Ueland, Chemical mismatch cleavage combined with capillary electrophoresis: detection of mutations in exon 8 of the cystathionine β-synthase gene, Clin. Chem. 44 (1998) 2108-2114.

(19) Y.-Q. Li, L.-Y. Guan, J.-H. Wang, H.-L. Zhang, J. Chen, S. Lin, W. Chen, Y.-D. Zhao, Simultaneous detection of dual single-base mutations by capillary electrophoresis using quantum dot-molecular beacon probe, Biosens. Bioelectron. 26 (2011) 2317-2322.

(20) A. Ganguly, D. J. Prockop, Detection of mismatched bases in double stranded DNA by gel electrophoresis, Electrophoresis 16 (1995) 1830-1835

(21) A.L. Børresen, Mismatch detection using heteroduplex analysis, Curr. Protoc. Hum. Genet. 7 (2002) 7.31-7.37.

(22) A.F. El-Yazbi, G.R. Loppnow. Detecting UV-induced nucleic-acid damage, Trends Anal. Chem. 61 (2014) 83-91.

(23) B. Dubertret, M. Calame, A. J. Libchaber, Single-mismatch detection using gold-quenched fluorescent oligonucleotides, Nature Biotech. 19 (2001) 365-370.

(24) R. Nutiu, Y. Li, Tripartite molecular beacons, Nucl. Acids Res. 30 (2002) e94.

(25) K. Yamana, Y. Ohshita, Y. Fukunaga, M. Nakamura, A. Maruyama, Bis-pyrene-labeled molecular beacon: A monomer–excimer switching probe for the detection of DNA base alteration, Bioorg. Med. Chem. 16 (2008) 78-83.

(26) C.-H. Lu, J. Li, J.-J. Liu, H.-H. Yang, X. Chen, G.-N. Chen, Increasing the Sensitivity and Single-Base Mismatch Selectivity of the Molecular Beacon Using Graphene Oxide as the "Nanoquencher", Chem. Eur. J. 16 (2010) 4889-4894.

(27) Y. Kam, A. Rubinstein, A. Nissan, D. Halle, E. Yavin, Detection of endogenous K-ras mRNA in living cells at a single base resolution by a PNA molecular beacon, Mol. Pharm. 9 (2012) 685-693.

(28) A.F. El-Yazbi, G.R. Loppnow, Chimeric RNA–DNA Molecular Beacons for Quantification of Nucleic Acids, Single Nucleotide Polymophisms, and Nucleic Acid Damage, Anal. Chem. 85 (2013) 4321-4327.

(29) N. Moran, D.M. Bassani, J.P. Desvergne, S. Keiper, P.A.S. Lowden, J.S. Vyle, H.R. Tucker, Detection of a single DNA base-pair mismatch using an anthracene-tagged fluorescent probe, Chem. Comm. 48 (2006) 5003-5005.

(30) T. Tedeschi, A. Tonelli, S. sforza, R. Corradini, R. Marchelli, A pyrenyl-PNA probe for DNA and RNA recognition: Fluorescence and UV absorption studies, Artif. DNA PNA XNA 1(2010) 83-89.

(31) Y. Huang, H.-Y. Yang, Y. Ai, DNA Single-Base Mismatch Study Using Graphene Oxide Nanosheets-Based Fluorometric Biosensors, Anal. Chem. 87 (2015) 9132-9136.

(32) P. Fu, C. Turro, Energy Transfer from Nucleic Acids to Tb(III): Selective Emission Enhancement by Single DNA Mismatches, J. Am. Chem. Soc. 121 (1999) 1-7.

(33) A.F. El-Yazbi, G.R. Loppnow, Terbium fluorescence as a sensitive, inexpensive probe for UV-induced damage in nucleic acids, Anal. Chim. Acta. 786 (2013) 116-123.

(34) D. Costa, H.D. Burrows, M. da Graça Miguel, Changes in Hydration of Lanthanide Ions on Binding to DNA in Aqueous Solution, Langmuir 21 (2005) 10492-10496.

(35) G. Yonuschot, G.W. Mushrush, Terbium as a fluorescent probe for DNA and chromatin, Biochemistry 14 (1975) 1677-1681.

(36) M.D. Topal, J.R. Fresco, Fluorescence of terbium ion-nucleic acid complexes: a sensitive specific probe for unpaired residues in nucleic acids, Biochemistry 19 (1980) 5531-5537.

(37) D.S. Gross, H. Simpkins, Evidence for Two-site Binding in the Terbium(II1)-Nucleic Acid Interaction, J. Biol. Chem. 256 (1981) 9593-9598.

(38) D. Jean-claude, A. Bunzli, H. Sigel, Luminescent Lanthanide Probes as Diagnostic and Therapeutic Tools. In: A. Sigel, H. Sigel (Eds.), Metal ions in biological systems, M. Dekker Inc. New York, 2004, 40-72.

(39) H. Simpkins, L.F. Pearlman, L.M. Thompson, Effects of Adriamycin on Supercoiled DNA and Calf Thymus Nucleosomes Studied with Fluorescent Probes, Cancer Res. 44 (1984) 613-618.

(40) K.T. Rim, K.H. Koo, J.S. Park, Toxicological Evaluations of Rare Earths and Their Health Impacts to Workers: A Literature Review, Saf. Health Work 4 (2013) 12-26

(41) J. Mérian, J. Gravier, F. Navarro, I. Texier, Fluorescent Nanoprobes Dedicated to in Vivo Imaging: From Preclinical Validations to Clinical Translation, Molecules 17 (2012) 5564-5591

(42) T. Naiser, J. Kayser, T. Mai, W. Michel, A. Ott, Position dependent mismatch discrimination on DNA microarrays—experiments and model, BMC Bioinformatics 9:509 (2008) 1-12

(43) H. Urakawa, P.A. Noble, S. El Fantroussi, J.J. Kelly, D.A. Stahl, Single-base-pair discrimination of terminal mismatches by using oligonucleotide microarrays and neural network analyses, Appl. Environ. Microbiol. 68 (2002) 235-244.

(44) S. Nakae, A. Hijikata, T. Tsuji, K. Yonezawa, K. Kouyama, K. Mayanagi, S. Ishino, Y. Ishino, T. Shirai, Structure of the EndoMS-DNA Complex as Mismatch Restriction Endonuclease, Structure 24 (2016) 1960-1971.

(45) S. Ishino, Y. Nishi, S. Oda, T. Uemori, T. Sagara, N. Takatsu, T. Yamagami, T. Shirai, Y. Ishino, Identification of a mismatch-specific endonuclease in hyperthermophilic Archaea, Nucl. Acids Res. 44 (2016) 2977-2986.

(46) M.L. Hegde, T. Izumi, S. Mitra, Oxidized base damage and single-strand break repair in mammalian genomes: role of disordered regions and posttranslational modifications in early enzymes, Prog. Mol. Biol. Transl. Sci. 110 (2012) 123-53.

(47) R. Owczarzy, A.V. Tataurov, Y. Wu, J.A. Manthey, K.A. McQuisten, H.G. Almabrazi, K.F. Pedersen, Y. Lin, J. Garretson, N.O. McEntaggart, C.A. Sailor, R.B. Dawson, A.S. Peek, IDT SciTools: A suite for analysis and design of nucleic acid oligomers, Nucl. Acids Res. 36 (2008) W163- W169.

(48) A. Rich, I. Tinoco, The effect of chain length upon hypochromism in nucleic acids and polynucleotides, J. Am. Chem. Soc. 82 (1960) 6409-6411.

(49) I. Tinoco, Hypochromism in Polynucleotides, J. Am. Chem. Soc. 82 (1960) 4785-4790.

(50) P. HaJeung, Z. Kaijiang, R. Yingjie, N. Sourena, S. Nanda, T. John-Stephen, K. ChulHee, Crystal structure of a DNA decamer containing a cis-syn thymine dimer, Proc. Natl. Acad. Sci. U. S. A. 99 (2002) 15965-15970.

(51) A.E. Rumora, K.M. Kolodziejczak, A.M.Wagner, M.E. Núñez, Thymine Dimer-Induced Structural Changes to the DNA Duplex Examined with Reactive Probes, Biochemistry 47 (2008) 13026-13035.

(52) A. Banyasz, S. Karpati, E. Lazzarotto, D. Markovitsi, T. Douki, UV-Induced Structural Changes of Model DNA Helices Probed by Optical Spectroscopy, J. Phys. Chem. C, 113 (2009) 11747-11750.

Table 1. Sequences of the ssDNA and hairpin probe used in this study.

Symbol	Sequence
S^{0}	5'-G T G C G A G G G A C T G T G C G-3' 1 2 3 4 5 6 7 8 9 10 11 12 13 14 15 16 17
S_{8}^{1}	5'-G T G C G A G **C** G A C T G T G C G-3'
S_{1}^{1}	5'-**C** T G C G A G G G A C T G T G C G-3'
S_{17}^{1}	5'-G T G C G A G G G A C T G T G C **C**-3'
S_{3}^{1}	5'-G T **C** C G A G G G A C T G T G C G-3'
S_{15}^{1}	5'-G T G C G A G G G A C T G T **C** C G-3'
S_{5}^{1}	5'-G T G C **C** A G G G A C T G T G C G-3'
S_{13}^{1}	5'-G T G C G A G G G A C T **C** T G C G-3'
$S_{8,9}^{2}$	5'-G T G C G A G **C C** A C T G T G C G-3'
$S_{1,8}^{2}$	5'-**C** T G C G A G **C** G A C T G T G C G-3'
$S_{1,3}^{2}$	5'-**C** T **C** C G A G G G A C T G T G C G-3'
$S_{1,17}^{2}$	5'-**C** T G C G A G G G A C T G T G C **C**-3'
$S_{1,3,8,9}^{4}$	5'-**C** T **C** C G A G **C C** A C T G T G C G-3'
$S_{1,3,15,17}^{4}$	5'-**C** T **C** C G A G G G A C T G T **C** C **C**-3'
hp probe	3'-*TCC GCG* GCA CGC TCC CTG ACA *CGC GGA*-5'

The superscript on the symbol represents the number of mismatched bases and the subscript number is the location of the mismatched base in the DNA, the bold bases represent the mismatched bases and the italicized bases represent the stem of the hp probe.

Table 2. Sequences of dsDNA used in this study.

Duplex	Sequence
D^{0}	5'- TGACGGCGCGAACCTAAGCTTAGCACTGACAGTCGATCAGTTGTCACGATCAGTAGCAATCGATCGTATATATGCGAAGATGCGCGGTAC- 3'
D^{14}_{39-52}	5'- TGACGGCGCGAACCTAAGCTTAGCACTGACAGTCGATC**TCAACAGTGCTAGT**GTAGCAATCGATCGTATATATGCGAAGATGCGCGGTAC- 3'
D^{26}_{33-58}	5'- TGACGGCGCGAACCTAAGCTTAGCACTGACAG**AGCTAGTCAACAGTGCTAGTCATCGT**ATCGATCGTATATATGCGAAGATGCGCGGTAC- 3'
D^{38}_{27-64}	5'- TGACGGCGCGAACCTAAGCTTAGCAC**ACTGTCAGCTAGTCAACAGTGCTAGTCATCGTTAGCTA**CGTATATATGCGAAGATGCGCGGTAC- 3'
D^{54}_{19-72}	5'- TGACGGCGCGAACCTAAG**GAATCGTGACTGTCAGCTAGTCAACAGTGCTAGTCATCGTTAGCTAGCATATAT**TGCGAAGATGCGCGGTAC- 3'
D^{60}_{16-75}	5'- TGACGGCGCGAACCT**TTCGAATCGTGACTGTCAGCTAGTCAACAGTGCTAGTCATCGTTAGCTAGCATATATACG**GAAGATGCGCGGTAC- 3'
D^{66}_{13-78}	5'- TGACGGCGCGAA**GGATTCGAATCGTGACTGTCAGCTAGTCAACAGTGCTAGTCATCGTTAGCTAGCATATATACGCTT**GATGCGCGGTAC- 3'
D^{72}_{10-81}	5'- TGACGGCGC**CTTGGATTCGAATCGTGACTGTCAGCTAGTCAACAGTGCTAGTCATCGTTAGCTAGCATATATACGCTTCTA**GCGCGGTAC- 3'
D^{74}_{9-82}	5'-TGACGGCG**GCTTGGATTCGAATCGTGACTGTCAGCTAGTCAACAGTGCTAGTCATCGTTAGCTAGCATATATACGCTTCTAC**CGCGGTAC-3'
D^{78}_{7-84}	5'TGACGG**GCGCTTGGATTCGAATCGTGACTGTCAGCTAGTCAACAGTGCTAGTCATCGTTAGCTAGCATATATACGCTTCTACGC**CGGTAC-3'
D^{84}_{4-87}	5'-TGA**GCCGCGCTTGGATTCGAATCGTGACTGTCAGCTAGTCAACAGTGCTAGTCATCGTTAGCTAGCATATATACGCTTCTACGCGCC**TAC -3'
C	3'-ACTGCCGCGCTTGGATTCGAATCGTGACTGTCAGCTAGTCAACAGTGCTAGTCATCGTTAGCTAGCATATATACGCTTCTACGCGCCATG -5'

D^{x} denotes a sequence containing 'x' mismatched bases, where the superscript number is the number of mismatched bases in the sequence and the subscript number is the range of location of the mismatched base in the DNA strand, C is the complementary DNA sequence to all the D^{x} sequences and underlined bold bases are the mismatched bases.

Table 3. Analytical Parameters for Quantification of Mismatch Detection

Parameter[a]	
Linear Dynamic Range (mismatches)	0 - 66
R^2	0.9986
Sensitivity (c.p.s. mismatch^{-1})	2.37×10^4
LOD (mismatches)	0.99
LOQ (mismatches)	3.3

For the determination of LOD and LOQ, the luminescence intensity of 5 solutions of D^0-Tb^{3+} were used as the background measurement. The standard deviations of these measurements were 0.782×10^4 c.p.s.

[a]In this table, linear dynamic range is the concentration range corresponding to the linear region in the calibration curve, R^2 is the linear regression coefficient squared, sensitivity is the slope of the calibration curve, LOD is the limit of detection and is 3 times the standard deviation of the background divided by the sensitivity, and LOQ is the limit of quantification and is 3.3 times the LOD.

Figure Legends

Figure 1. The luminescence spectra of 40 μM Tb^{3+} and 1 μM ssDNA sequence S^0 in the absence (—) and presence (…) of 1 μM complementary hp probe (40 mM Tris, 10 mM NaCl, pH 7.5). The fluorescence excitation wavelength was 280 nm and the spectra were recorded at room temperature. "c.p.s." denotes counts per second.

Figure 2. Tb^{3+} luminescence intensity (λ_{ex}=280 nm, λ_{em}=545 nm) as a function of the number and the location of mismatches in a 17-mer DNA oligonucleotide sequences in the presence of the hp probe. The location is determined from the 5' end of the 17-mer DNA oligonucleotide sequences. The measurements were recorded at room temperature. "c.p.s." denotes counts per second.

Figure 3. (A) Calculated [47] T_m vs. number of mismatches for different mismatched dsDNA sequences. White stars represent mismatched sequences used in this study and their sequences are shown in Table 2. The inner plot shows the melting temperatures for sequences containing 0 to 80 mismatches, which have $T_m \geq 0$ °C. (B) The Tb^{3+} luminescence intensity (λ_{ex}= 280 nm, λ_{em}= 545 nm) of the dsDNA mismatched sequences annealed twice. (C) Absorbance measurements at 260 nm versus the number of mismatches of the twice-annealed dsDNA mismatched sequences. Each data point is an average of three replicate measurements and the error bars correspond to the standard deviation of the measurements. "c.p.s." denotes counts per second.

Figure 4. Tb^{3+} luminescence intensity (λ_{ex} = 280 nm, λ_{em} = 545 nm) as a function of exposure time of ctDNA to UVC light at room temperature. Results from both the irradiated ctDNA

samples (filled squares) and the unirradiated control duplex (open circles) are shown. Tb^{3+} was added to the aliquots after irradiation. The solid line through the irradiated sample data points is a single-exponential growth fit to $I_L = I_{L,0} + a(1-e^{-t/\tau})$, where $I_{L,0} = (0.30 \pm 0.04)\ 10^5$ c.p.s., $a = 9.6 \pm 0.01$, and $\tau = 66.42 \pm 4.13$ min, The control points (open circles) are fit to a straight dotted line with zero slope by eye.

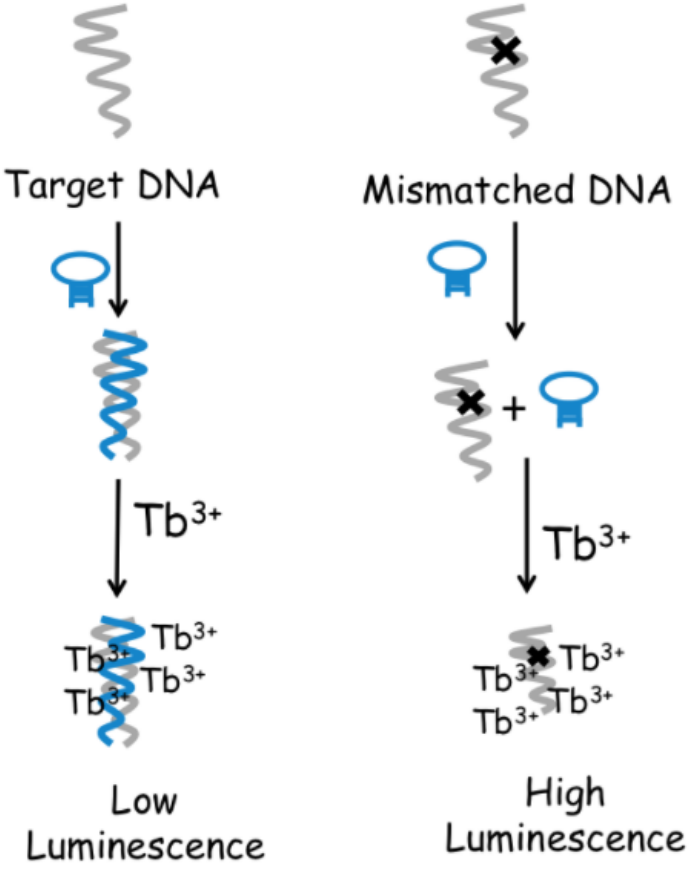

Scheme 1. Visual representation of the experiment. The target/mismatched DNA oligomers are hybridized with the complementary hairpin (hp), but the hybridization occurs less with the mismatched DNA oligo due to its lower T_m. After hybridization, Tb3+ is added to each solution, but binds in a more luminescent configuration with the guanines in the mismatched strand, leading to higher-intensity emission.

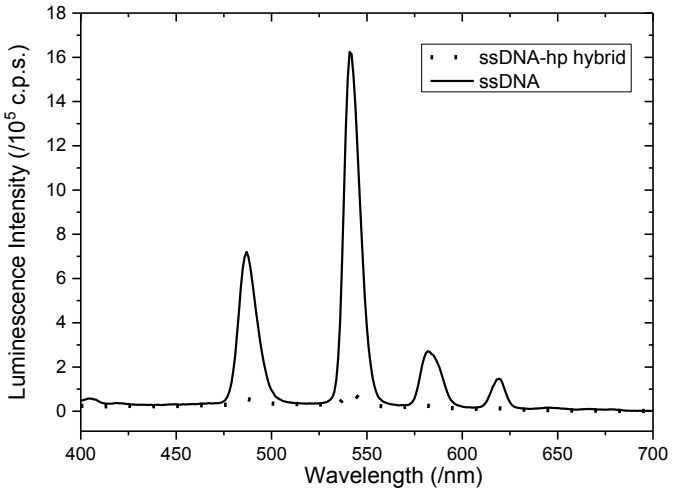
ssDNA-hp hybrid
ssDNA
Luminescence Intensity (/10^5 c.p.s.)
Wavelength (/nm)
0
2
4
6
8
10
12
14
16
18
400
450
500
550
600
650
700

Figure 1

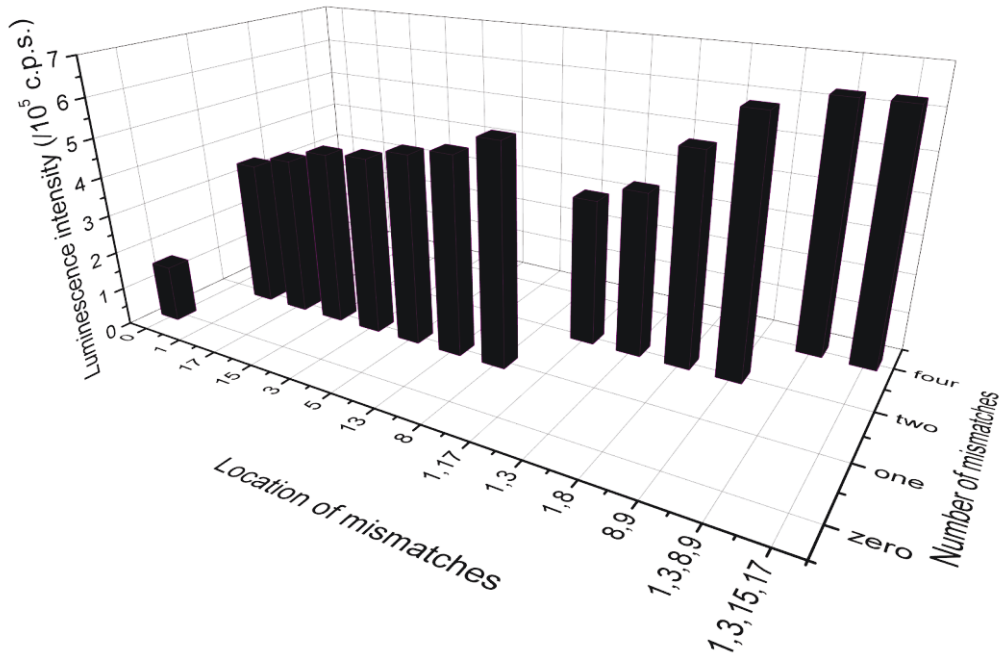
Luminescence intensity (/10^5 c.p.s.)
0
1
2
3
4
5
6
7
Location of mismatches
0
17
15
3
5
13
8
1,17
1,3
1,8
8,9
1,3,8,9
1,3,15,17
Number of mismatches
four
two
one
zero

Figure 2

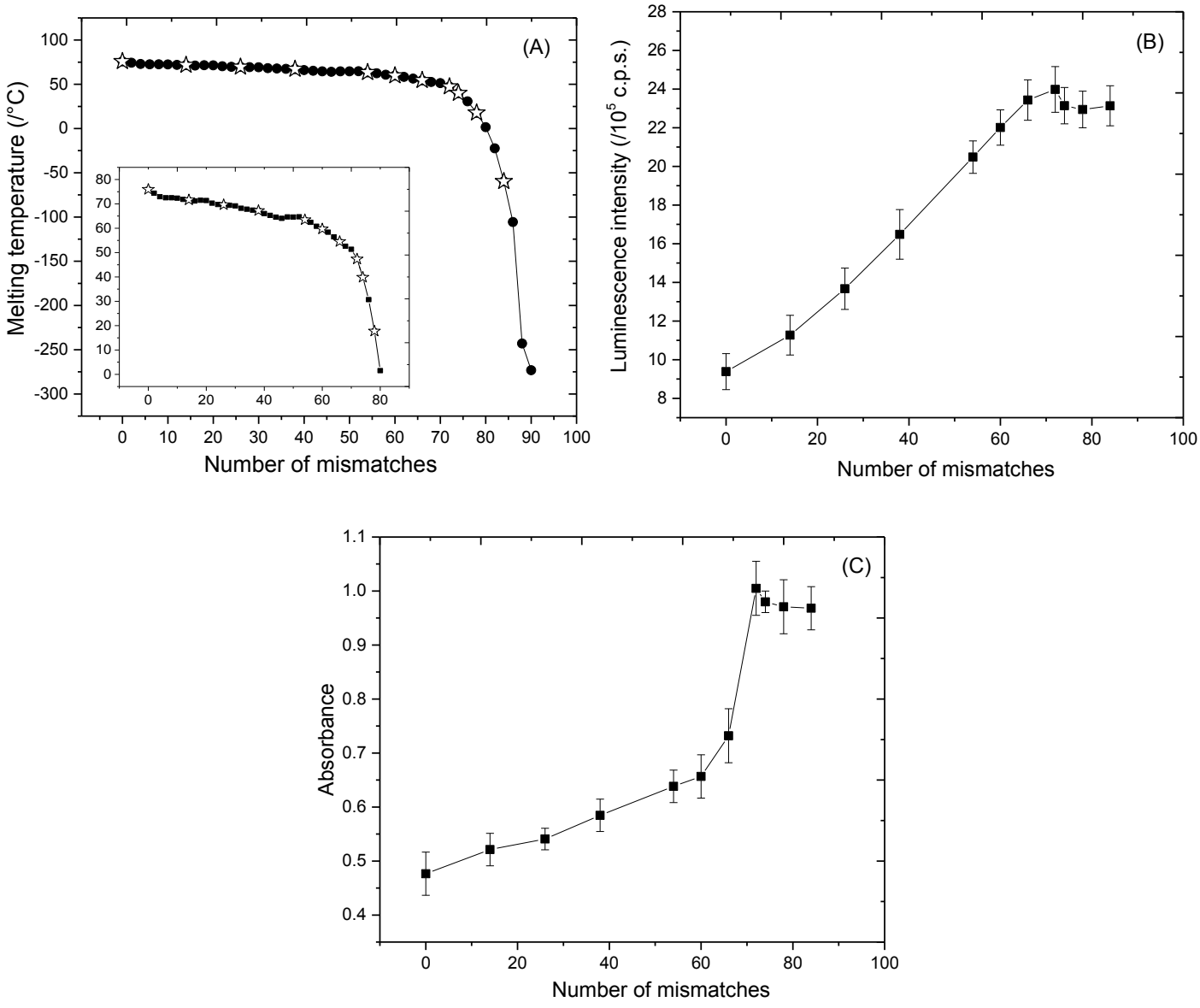
(A)
Melting temperature (/°C)
Number of mismatches
(B)
Luminescence intensity (/10^5 c.p.s.)
Number of mismatches
(C)
Absorbance
Number of mismatches

Figure 3

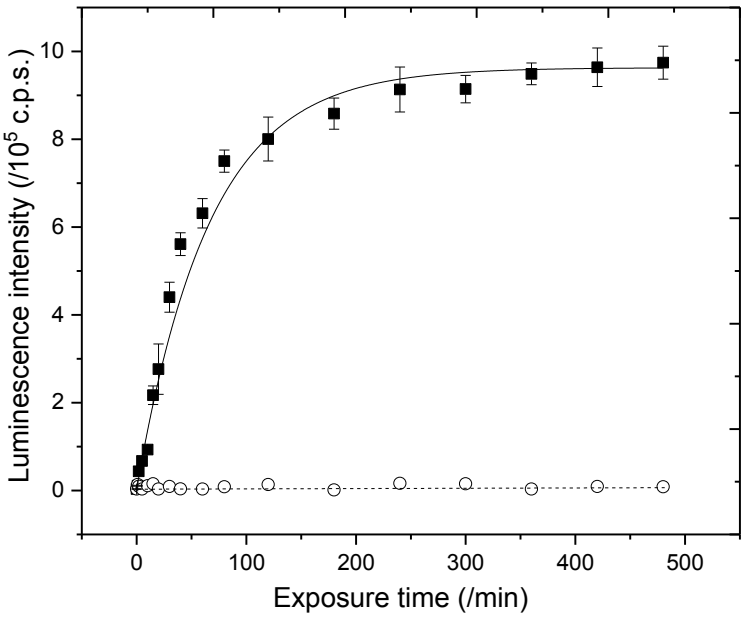
Luminescence intensity (/10^5 c.p.s.)
0
2
4
6
8
10
0
100
200
300
400
500
Exposure time (/min)

Figure 4